NASA TECHNICAL MEMORANDUM

NASA TM X-3363

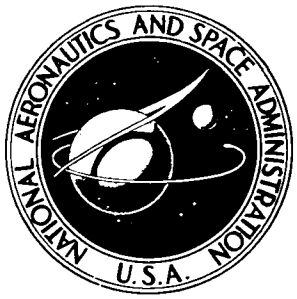

NASA TM X-3363

AN EVALUATION OF THE METHOD FOR DETERMINING THE WHITHAM F-FUNCTION USING DISTRIBUTIONS OF DOWNWASH AND SIDEWASH ANGLES

Joel P. Mendoza and Raymond M. Hicks

Ames Research Center
Moffett Field, Calif. 94035

NATIONAL AERONAUTICS AND SPACE ADMINISTRATION • WASHINGTON, D. C. • MARCH 1976

1. Report No.	2. Government Accession No.	3. Recipient's Catalog No.
NASA TM X-3363		

4. Title and Subtitle	5. Report Date
AN EVALUATION OF THE METHOD FOR DETERMINING THE WHITHAM F-FUNCTION USING DISTRIBUTIONS OF DOWNWASH AND SIDEWASH ANGLES	March 1976
	6. Performing Organization Code
7. Author(s)	8. Performing Organization Report No.
Joel P. Mendoza and Raymond M. Hicks	A-6228
	10. Work Unit No.
9. Performing Organization Name and Address	505-10-12
NASA Ames Research Center Moffett Field, Calif. 94035	11. Contract or Grant No.
	13. Type of Report and Period Covered
12. Sponsoring Agency Name and Address	Technical Memorandum
National Aeronautics and Space Administration Washington, D. C. 20546	14. Sponsoring Agency Code

15. Supplementary Notes

16. Abstract

The method (due to Landahl *et al.*) of computing the Whitham F-function using distributions of downwash and sidewash angles was evaluated with two different models. F-functions which were calculated for a 4° (half angle) cone cylinder at M_∞ = 2.01, using theoretically and experimentally derived flow angles, show that the method of Landahl *et al.* is sensitive to small inaccuracies in the measured flow angles. An oblique wing transport model was tested at 0° angle of attack at M_∞ = 2.01. In this test, two different probes were used at two different distances from the model (one probe measured flow angularity and the other static pressures). The pressure signature derived from the F-function (computed using distributions of downwash and sidewash angles measured at the distance of 0.32 body lengths) was extrapolated and compared to the pressure signature measured at the distance of 0.87 body lengths with the static pressure probe. The agreement between the two pressure signatures is poor, and the discrepancy is believed to be due largely to the many inaccuracies involved in using a probe designed to measure flow angularity.

17. Key Words (Suggested by Author(s))	18. Distribution Statement
Sonic boom Pressure signatures Downwash angle Sidewash angle	Unlimited STAR Category - 02

19. Security Classif. (of this report)	20. Security Classif. (of this page)	21. No. of Pages	22. Price*
Unclassified	Unclassified	23	$3.25

*For sale by the National Technical Information Service, Springfield, Virginia 22161

SYMBOLS

F	F-function
h	altitude or vertical distance of the model or airplane above the measuring station, a function of the unit Heaviside step function
l	reference length
M	Mach number
p	static pressure
p_t	total pressure
R	radius of the equivalent body of revolution
S	cross-sectional area of the equivalent body of revolution
t	variable of integration
v	perturbation velocity in the r-direction
x,r,θ	cylindrical coordinates
x'	variable of integration
y	distance along the abscissa of the F-function
γ	ratio of the specific heats
ϵ	angle of downwash
θ_w	shock wave angle
Δp	sonic boom overpressure
σ	angle of sidewash
$( )'$	first derivative

Subscripts

0	zero, equation 5
1	quantity ahead of the normal shock and behind the oblique shock (see appendix)
2	quantity behind the normal shock (see appendix)
∞	free stream

AN EVALUATION OF THE METHOD FOR DETERMINING THE WHITHAM F-FUNCTION USING DISTRIBUTIONS OF DOWNWASH AND SIDEWASH ANGLES

Joel P. Mendoza and Raymond M. Hicks

Ames Research Center

SUMMARY

The method (due to Landahl *et al.*) of computing the Whitham F-function using distributions of downwash and sidewash angles was evaluated with two different models. F-functions which were calculated for a 4° (half angle) cone cylinder at $M_\infty = 2.01$, using theoretically and experimentally derived flow angles, show that the method of Landahl *et al.* is sensitive to small inaccuracies in the measured flow angles. An oblique wing transport model was tested at 0° angle of attack at $M_\infty = 2.01$. In this test, two different probes were used at two different distances from the model (one probe measured flow angularity and the other static pressures). The pressure signature derived from the F-function (computed using distributions of downwash and sidewash angles measured at the distance of 0.32 body lengths) was extrapolated and compared to the pressure signature measured at the distance of 0.87 body lengths with the static pressure probe. The agreement between the two pressure signatures is poor, and the discrepancy is believed to be due largely to the many inaccuracies involved in using a probe designed to measure flow angularity.

INTRODUCTION

A method, based on the Whitham theory (ref. 1), for predicting the overpressure characteristics of aircraft flying at supersonic speeds was presented by Hicks and Mendoza in reference 2. In this method, ground overpressure characteristics are determined by extrapolating the static pressures measured in the near field of a model tested in the wind tunnel. Since only a single configuration at one Mach number was investigated in reference 2, it was felt that further evaluation of the method was necessary. In the evaluation, data were used from a number of wind-tunnel tests conducted on a wide variety of model shapes at Mach numbers ranging from 1.68 to 4.63. In each case, data measured at one distance were extrapolated and compared to data measured at larger distances in the wind tunnel and, in each case, the agreement was excellent. These results are presented in references 3 and 4.

During the evaluation period of the Whitham-based method (ref. 2), an effort was underway by Landahl *et al.* to develop a different method for computing the F-function from experimental data which would include higher order terms neglected by the Whitham theory. This method, together with its applications to an axisymmetric body, was presented in reference 5. Further developments of this method were presented in reference 6 which showed that, in

order to include the higher order terms, distributions of downwash and sidewash angles for several roll angles must first be obtained. Using the method of reference 6, Ferri *et al.* (ref. 7) computed the sonic boom for a clipped-tip delta-wing/body configuration. Their predicted sonic boom level appeared to be lower than any previously presented on a similar wing/body configuration. And to verify this, calculations were performed using the alternate form for the Whitham F-function expression of reference 2. It is expressed as a function of the downwash angle ε instead of $\Delta p/p$. The sonic boom level given by this method, although considerably higher than Ferri's value, was consistent with previously reported data (ref. 8). As a result, an investigation was conducted to resolve the differences in sonic boom levels given by the two different methods and to determine if a pressure signature (computed from the F-function given by the method of ref. 6) can be extrapolated to larger distances. The results of the investigation are presented in this report.

MODELS AND APPARATUS

The models and the flow-angle probe of the present investigation conducted in the 20-Inch Supersonic Wind Tunnel at the Jet Propulsion Laboratory are described herein together with two models used in previously reported investigations. A description of the 20-Inch Supersonic Wind Tunnel is contained in reference 9.

Probe

Because of the favorable results obtained with the flow angle probe used in references 6, 7, and 10, a similar probe was constructed for use in the present investigation. The flow-angle probe, shown in figure 1, was manufactured by joining together three different components; namely the hemispherical tip, the transition section, and the probe afterbody. The hemispherical tip was constructed by inserting five small stainless steel tubes within a 2.77-mm (inside diameter) tube. The five small tubes, together with spacers, were silver soldered in place and ground to the desired hemispherical shape. The transition section (made of brass and configured to a truncated cone cylinder) was soldered to the probe tip and, in turn, soldered to the stainless steel (17-4PH) probe afterbody. In addition to the flow-angle probe, a static-pressure probe was used in the present investigation. Details of the static-pressure probe can be found in reference 2.

Wedge

Shown in figure 2 is the 6° (half angle) wedge which was used to calibrate the flow angle probe. The wedge, which was constructed of steel, was aligned with the centerline of the wind tunnel and fixed to the sidewalls of the test section of the JPL wind tunnel.

Cone Cylinder

Shown in figure 3 is the 4° (half angle) cone cylinder which also was used to calibrate the flow-angle probe. It was mounted on a linear actuator so that it could travel longitudinally along a line parallel to the centerline of the test section.

Transport Model

A sketch of the oblique-wing transport model is shown in figure 4. The model, although lacking engine pods, is complete with wings and empennage and was constructed of steel.

Other Models

Two models which were tested in previous investigations are the 3.24° (half angle) cone cylinder model (ref. 4) and the clipped-tip delta-wing/body model (ref. 7). Sketches of these models are shown in figures 5 and 6, respectively. Results from references 4 and 7 for these two models are discussed in a later section.

TEST PROCEDURES

In order to compute the F-functions for arbitrary model shapes, using the method of reference 6, distributions of downwash and sidewash angles must be obtained for several model roll angles. The flow angles are determined on the surface of an imaginary cylinder enclosing the model. The model reference point is located on the axis of the cylinder which is parallel to the flow. The radius of the cylinder is less than one body length. In this investigation, the instrument used for measuring flow angles was the flow-angle hemispherical probe (fig. 1). Calibrations and accuracy determinations for the hemispherical probe, together with measurements of the distributions of downwash and sidewash angles for the oblique-wing transport model, are discussed in the following sections. Standard sonic-boom testing technique using a static-pressure probe (refs. 4, 8, 11) were also used with one of the models in this test (the oblique-wing transport model).

Probe Calibration and Accuracy

The procedures used in calibrating the flow-angle probe are similar to those reported in reference 10 and are described briefly herein. Probe calibrations were made by measuring pressures at each of the five orifices of the probe at different probe pitch-and-roll angles. The probe was calibrated at each of the following survey Mach numbers: 1.48, 2.01, 2.62, and 3.27. At each Mach number, the probe was rolled from 0° to 180° in 10° increments and, at each roll angle, the probe was pitched from -5° to 5° in 1° increments.

Although the probe calibration procedures were similar to that of reference 10, the accuracy determinations were different. Probe accuracy was determined in the present investigation by making comparisons between the flow angles determined from probe measurements and those given by exact inviscid solutions to supersonic flows over wedges and cones.

To establish the accuracy of the probe for determining flow angles in a simple two-dimensional flow field, the probe was placed in the flow field of a 6° (half angle) wedge at the test Mach numbers of 2.01, 2.62, and 3.27. The probe was pitched by 1° increments from -7° to 0°. It is noted that when the probe is pitched to -6°, the probe axis is parallel to the surface of the wedge. The boundary-layer effects were initially neglected. Later, better agreement between the experimentally and theoretically derived wedge flow angles was obtained by applying flow-angle corrections due to boundary-layer-displacement thickness. This result is further discussed in the next section.

To establish the accuracy of the probe for determining flow angles in a simple axisymmetric flow field, probe pressure measurements of the distribution of downwash angles for a 4° (half angle) cone cylinder were made at Mach 2.01. To obtain the distribution of downwash angles, the cone cylinder model was mounted on a linear actuator which permitted the model to be moved longitudinally along a line parallel to the centerline of the test section. The probe was mounted on spacers fixed to the floor of the test section. This permitted the probe to be aligned longitudinally with the centerline of the wind tunnel.

Flow Field of the Oblique-Wing Transport Model

Using the same general arrangement of model and probe used in the cone cylinder case, distributions of downwash and sidewash angles for the oblique-wing transport model were obtained from probe pressure measurements made at Mach number 2.01. These flow angle distributions were obtained at each 5° increment in model roll angle from -5° to 25°. The model was at 0° angle of attack and at the distance of 0.32 body lengths (88.128 mm) from the probe. To measure the flow-field static-pressure distribution (pressure signature) for the oblique-wing transport model, a 2° (included angle) conical static probe was used in place of the hemispherical probe. Because the method of reference 2 has been previously shown (ref. 3) to be applicable to distances as close as 1 body length, the distance between the model and the static probe was increased from 0.32 to 0.87 body lengths, the maximum distance obtainable that was free of reflected shocks. The pressure signature measured at this distance has been compared to the pressure signature obtained from the F-function computed from the method of reference 6 and is discussed in a later section.

RESULTS AND DISCUSSION

Theory

Whitham's expression (ref. 1) for nonsmooth axisymmetric bodies is

$$\left.\begin{aligned} F &= \frac{1}{2\pi}\int_0^{\infty}\left[\frac{2}{\beta R(t)}\right]^{1/2} h\left[\frac{y - t}{\beta R(t)}\right] dS'(t) \\ y &= x - \beta r + kFr^{1/2} \end{aligned}\right\} \qquad (1)$$

where

$$\beta = (M_\infty{}^2 - 1)^{1/2} \quad \text{and} \quad k = (\gamma + 1)M_\infty{}^4/2^{1/2}\beta^{3/2}$$

Pressure signatures are computed using the expressions

$$\left.\begin{aligned} \frac{\Delta p}{p} &= \frac{\gamma M_\infty{}^2}{(2\beta r)^{1/2}} F \\ x - \beta r &= y - kFr^{1/2} \end{aligned}\right\} \qquad (2)$$

Hicks and Mendoza (ref. 2) computed F-functions using experimentally derived values of $\Delta p/p$. They rearranged expression (2) in the form

$$\left.\begin{aligned} F &= \frac{(2\beta r)^{1/2}}{\gamma M_\infty{}^2}\frac{\Delta p}{p} \\ y &= x - \beta r + kFr^{1/2} \end{aligned}\right\} \qquad (3)$$

The data (refs. 2 and 3) indicate that these expressions are applicable to distances as close to the model as one body length. An alternate form for F is

$$\left.\begin{aligned} F &= \left(\frac{2r}{\beta}\right)^{1/2} v \\ y &= x - \beta r + kFr^{1/2} \end{aligned}\right\} \qquad (4)$$

where

$$v = \beta\varepsilon/(\beta + \varepsilon)$$

In this report, Hicks and Mendoza used this expression and data from reference 7 to compute the ground-level sonic boom for Ferri's clipped-tip delta-wing/body model. Ferri, on the other hand, used Landahl's expression

$$F = \left(\frac{2r_0}{\beta}\right)^{1/2}\left(v + \frac{3\phi}{r_0} - \frac{1}{2}\frac{\partial^2\phi}{\partial\theta^2}\right)$$

$$y = x - \beta r + kFr^{1/2} + \left(M_\infty{}^2 - \frac{K}{4}\right)\phi - K\frac{\partial^2\phi}{\partial\theta^2} \qquad (5)$$

where

$$v = \frac{\beta\varepsilon}{\beta + \varepsilon}$$

$$K = \frac{K}{(2\beta)^{1/2}}$$

$$r_0 = r\left(1 - \frac{K\varepsilon}{\beta}\right)$$

$$\phi = -\frac{1}{\beta}\int_0^x \varepsilon(x')\,dx'$$

$$\frac{\partial^2\phi}{\partial\theta^2} = r\frac{d\sigma}{d\theta}$$

Measurements of Downwash and Sidewash Angles

Figure 7 shows measured and corrected downwash angles at Mach number 2.7. Corrections (described in ref. 7) to the measured downwash are applied only to those measured in the vicinity of the shockwaves generated by the model. Because of the angle of the shock and the thickness of the pressure probe, one set of probe orifices may lie in the flow-field region upstream of the shock, while the remainder of the orifices may lie in the downstream region from the shock. The flow angle computed in this case, doubtlessly, will be in error, since the probe calibrations are not applicable. The flow-angle probe can only be used in the flow regions between shocks. Schlieren photographs were used for locating those flow angles measured near the shocks. The correction process, as described in reference 7, is to simply discard those flow angles measured at or near the shock. However, because the shock waves appear on the schlieren photographs as having finite thickness, some uncertainty is introduced in selecting which flow angles are to be discarded.

Sidewash angles used to calculate $\partial^2\phi/\partial\theta^2 = r\,d\sigma/d\theta$ are shown in figure 8 for two different longitudinal stations in the wind tunnel. The slope $d\sigma/d\theta$ is taken at the required value of θ. For example, the slope $d\sigma/d\theta$ is evaluated at $\theta = 0^\circ$ for computing the overpressures directly beneath an airplane in straight and level flight. The method employed in reference 7 is to fair a curve through the data points and to take the slope of the curve at $\theta = 0^\circ$. However, obtaining values of $d\sigma/d\theta$ with a high degree of credibility is difficult, since considerable scatter often exists in the data.

Pressure Signatures From Reference 7

Pressure signatures were computed using both expressions (4) and (5), from Whitham and Landahl, respectively. These are compared in figure 9 to show the effects of neglecting the higher order terms. Curve 1 was computed using the alternate form of the Whitham expression (eq. (4)) and the measured downwash angles given in reference 7. Whitham's alternate form was used because of the availability of measured downwash angles. No attempt was made, however, to correct the measured downwash angles by the method described in reference 7, because of the uncertainty in selecting which data points to discard. Curves 2 through 4 were derived from F-functions computed by the Landahl method. Because of model symmetry about the $\theta = 0^\circ$ plane, the distributions of sidewash angles, σ versus θ, would be expected to show symmetry about the point $\theta = 0^\circ$ at all x-stations. The F-function in this case would not include contributions from the term $\partial^2\phi/\partial\theta^2$, because $d\sigma/d\theta = 0$ at $\theta = 0^\circ$. Curve 2 does not include the $\partial^2\phi/\partial\theta^2$ term, and it is interesting to note the similarity between the curves 1 and 2 computed using the methods of Whitham and Landahl *et al.*, respectively. F-functions given in reference 7 were used to compute curves 3 and 4. Curve 4 is the pressure signature whose F-function has been corrected by an area-balancing method proposed in reference 7 to eliminate multiple values of the F-function. The apparent effect on the pressure signature of neglecting the term containing ϕ (eq. (5)) is small, as shown by the comparisons of curves 1 and 2. However, by imposing nonzero values of $\partial^2\phi/\partial\theta^2$ in the F-function calculations (as suggested by Ferri *et al.*) a reduction in area in the expansion region behind the shock wave of the wing at angle of attack is observed (curve 3). As a result, curve 3 differs substantially from both curves 1 and 2. This difference in areas, as shown later, accounts for the large difference in the predicted ground overpressure characteristics. Also the effect of the F-function area balancing (ref. 7) further reduces the maximum ground overpressure. The effects of the different near-field pressure signatures (fig. 9) on the predicted ground overpressures given by the extrapolation method of reference 12 are illustrated in figure 10. Curves 1 and 2 are observed to agree well with each other, wereas curves 1, 3, and 4 are entirely different from one another. This is noted particularly in the large differences in both the shock strength and wing-shock location.

Present Investigation

No attempt was made in reference 7 to extrapolate pressure signatures from one distance to larger distances in the wind tunnel. Therefore, a wind-tunnel investigation was conducted to determine whether the pressure signature derived from the F-function (from Landahl *et al.*) could be extrapolated to large distances. This investigation was conducted in the 20-Inch Supersonic Wind Tunnel at the Jet Propulsion Laboratory. The flow angle probe was calibrated for survey Mach numbers 1.48, 2.01, 2.62, and 3.27 at 132.69 kN/m^2 total pressure. The accuracy of the flow-angle probe is demonstrated by flow-angle measurements in the flow fields of a 6° (half angle) wedge and a cone cylinder for which exact inviscid flow-field solutions exist. The 6° (half angle) wedge was tested at Mach numbers of 2.01, 2.62, and 3.27 at 132.69 kN/m^2 total pressure. The measurements of the downwash angles are shown in figure 11.

Also presented in the figure are downwash angles obtained from total pressure measurements and by iteration of the oblique shock relations. Both the measured and calculated flow angles are observed to be somewhat greater than the expected value of 6.1° (6° wedge half angle plus 0.1° for the boundary-layer-displacement thickness). The discrepancy remains unexplained at this time. Because the wedge was aligned with the centerline of the test section and was not instrumented to permit the determination of the "wind on" angle of attack directly, the actual wedge-flow deflection angle was determined by using the oblique shock relations (ref. 13) as described in the appendix.

To demonstrate the accuracy of the probe for use in simple axisymmetric flow fields, F-functions computed from measured and theoretically derived downwash angles, and by the Whitham theory (see eq. (1)) for a 4° (half-angle) cone cylinder at Mach number 2.01 are shown in figure 12. The measured downwash angles give higher values of F than those calculated by the two other methods, which agree closely with one another. Thus the calculation of the F-function by the method of Landahl *et al.* appears quite sensitive to the small errors in the measured downwash angles. Similar results using the standard sonic-boom experimental technique of measuring static pressures are shown in figure 13. Here the F-function for a 3.24° (half angle) cone cylinder at Mach number 1.68 is computed from static-pressure measurements (eq. (2)) and from the Whitham theory (eq. (1)) using exact expressions for the cone-cylinder cross-sectional area distribution. Agreement is good except in the region of the bow shock wave, where smearing of the pressures, due to model and probe vibration and stream turbulence, is apparent. (The smearing phenomenon is discussed in detail in ref. 11.)

Extrapolation of Pressure Signature

A comparison of measured and extrapolated overpressure characteristics for the 3.24° (half angle) cone cylinder is shown in figure 14. Data measured at a distance of 10 cone lengths were extrapolated (using the method of ref. 2) and compared to data measured at a distance of 20 cone lengths. Good agreement is noted, except in the region of the bow shock, because of smearing of the measured pressures.

Oblique-Wing Transport Model

To determine whether the F-function (calculated from flow angles measured in the near field) can be used to predict overpressure characteristics measured at a larger distance, an oblique-wing transport model at 0° angle of attack was tested at Mach number 2.01 with 132.69 kN/m^2 total pressure. Since this model is highly asymmetric, the $\partial^2\phi/\partial\theta^2$ term would be expected to be different from zero at $\theta = 0°$. Two pressure signatures, one derived from an F-function which was computed from flow-angle measurements and the other from static pressure measurements are shown in figure 15. The pressure signature computed from the F-function derived from flow angles measured at a distance of 0.32 body lengths was extrapolated and compared to the pressure signature measured with a static pressure probe at the distance of 0.87 body lengths.

The agreement is considered poor and the discrepancies shown between the two pressure signatures are believed to be largely due to the inaccuracy of the probe measurements.

Advantages and Disadvantages of the Two Methods

Method from reference 2— The advantages of this method are: (a) it is a simple experimental technique, (b) no corrections to the data are necessary, and (c) the technique is demonstrated to be reliable and accurate (see refs. 3 and 4). The only disadvantage, for most configurations, is the near-field pressure signature must be measured at the distance of at least one body length from the model. This is not considered to be a serious limitation of the method.

Method from reference 6— The advantage of this method may be that measurements can be made at small distances from the model. This would permit the use of large models and/or small wind tunnels. However, there are several serious disadvantages of this method: (a) corrections must be applied to the measured downwash angles before calculating the F-function, (b) the numerical differentiation of the sidewash angles is difficult to perform accurately, and (c) it is a complicated experimental technique which involves difficult measurements of the downwash and sidewash angles.

CONCLUSIONS

While the method of reference 6 has the advantage of permitting measurements to be made close to the model, it has several disadvantages. It is sensitive to small inaccuracies in the measured flow angles. It requires derivatives of the sidewash angles which are difficult to obtain because considerable scatter often exist in the measured data. Flow angles in the vicinity of shock waves cannot be accurately measured, making it necessary to correct the distributions of downwash and sidewash angles before the F-function can be calculated. And the most serious drawback in the method of reference 6 is its complexity. It is more difficult to apply than the method of reference 2. The poor agreement between the measured and extrapolated data for the oblique-wing transport model is believed to be largely due to the inaccuracies in the measured flow angles.

Ames Research Center
National Aeronautics and Space Administration
Moffett Field, Calif. 94035, Sept. 8, 1975

APPENDIX A

ITERATIVE METHOD FOR DETERMINATION OF FLOW TURNING ANGLE

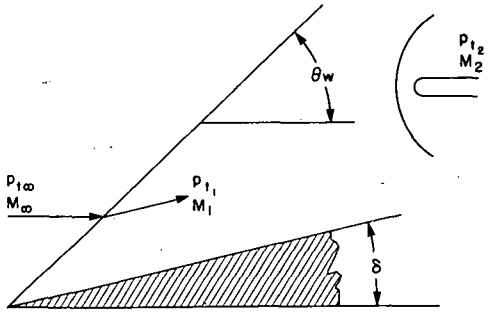

Sketch of flow quantities.

$$\frac{p_{t_1}}{p_{t_\infty}} = \left(\frac{6M_\infty^2 \sin^2 \theta_w}{M_\infty^2 \sin^2 \theta_w + 5}\right)^{7/2} \left(\frac{6}{7M_\infty^2 \sin^2 \theta_w - 1}\right)^{5/2} \tag{A1}$$

$$\frac{p_{t_2}}{p_{t_1}} = \left(\frac{6M_1^2}{M_1^2 + 5}\right)^{7/2} \left(\frac{6}{7M_1^2 - 1}\right)^{5/2} \tag{A2}$$

$$M_1^2 = \frac{36M_\infty^4 \sin^2 \theta_w - 5(M_\infty^2 \sin^2 \theta_w - 1)(7M_\infty^2 \sin^2 \theta_w + 5)}{(7M_\infty^2 \sin^2 \theta_w - 1)(M_\infty^2 \sin^2 \theta_w + 5)} \tag{A3}$$

All three of the preceding expressions (eqs. (A1)-(A3)) are used in the following expression

$$\frac{p_{t_2}}{p_{t_\infty}} - \left(\frac{p_{t_1}}{p_{t_\infty}}\right)\left(\frac{p_{t_2}}{p_{t_1}}\right) = 0 \tag{A4}$$

Equation (A4) is a function of θ_w alone, since M_∞, p_{t_∞} and p_{t_2} are known quantities. An iteration on θ_w is performed until equation (A4) is satisfied. With θ_w known, the wedge angle is obtained from the expression

$$\tan \delta = \frac{5 \cot \theta_w (M_\infty^2 \sin^2 \theta_w - 1)}{5 + M_\infty^2 (6 - 5 \sin^2 \theta_w)} \tag{A5}$$

REFERENCES

1. Whitham, G. B.: The Flow Pattern of a Supersonic Projectile. Commun. Pure. Appl. Math., vol. V, no. 3, Aug. 1952, pp. 301-348.

2. Hicks, Raymond M.; and Mendoza, Joel P.: Prediction of Aircraft Sonic Boom Characteristics from Experimental Near Field Results. NASA TM X-1477, 1967.

3. Mendoza, Joel P.; and Hicks, Raymond M.: Further Studies of the Extrapolation of Near Field Overpressure Data. NASA TM X-2219, 1971.

4. Mendoza, Joel P.; and Hicks, Raymond M.: On the Extrapolation of Measured Near Field Pressure Signatures of Unconventional Configurations. NASA SP-255, 1971, pp.385-392.

5. Landahl, M. T.; Ryhming, I. L.; and Hilding, L.: Nonlinear Effects on Sonic Boom Intensity. NASA SP-180, 1968, pp.117-124.

6. Landahl, M.; Ryhming, I.; Sorensen, H.; and Drougge, G.: A New Method for Determining Sonic Boom Strength from Near-Field Measurements. NASA SP-255, 1971, pp. 285-295.

7. Ferri, A.; Wang, Huai-Chu; and Sorensen, Hans: Experimental Verification of Low Sonic Boom Configuration. NASA CR-2070, June 1972.

8. Hunton, Lynn W.; Hicks, Raymond M.; and Mendoza, Joel P.: Some Effects of Wing Planform on Sonic Boom. NASA TN D-7160, 1973.

9. Staff of the Aerodynamics Facilities Section: Jet Propulsion Laboratory Wind Tunnel Facilities, JPL Techincal Memorandum 33-335, April 1, 1967.

10. Sorensen, Hans: Device for Measurement of the Supersonic Flow Field. The Aeronautical Institute of Sweden, FFAP-A-279, Sept. 1972.

11. Carlson, Harry W.: Correlation of Sonic Boom Theory with Wind Tunnel and Flight Measurements. NASA TR R-213, 1964.

12. Thomas, Charles L.: Extrapolation of Sonic Boom Pressure Signatures by the Waveform Parameter Method. NASA TN D-6832, 1972.

13. Ames Research Staff: Equations, Tables, and Charts for Compressible Flow. NACA Rept. 1135, 1953.

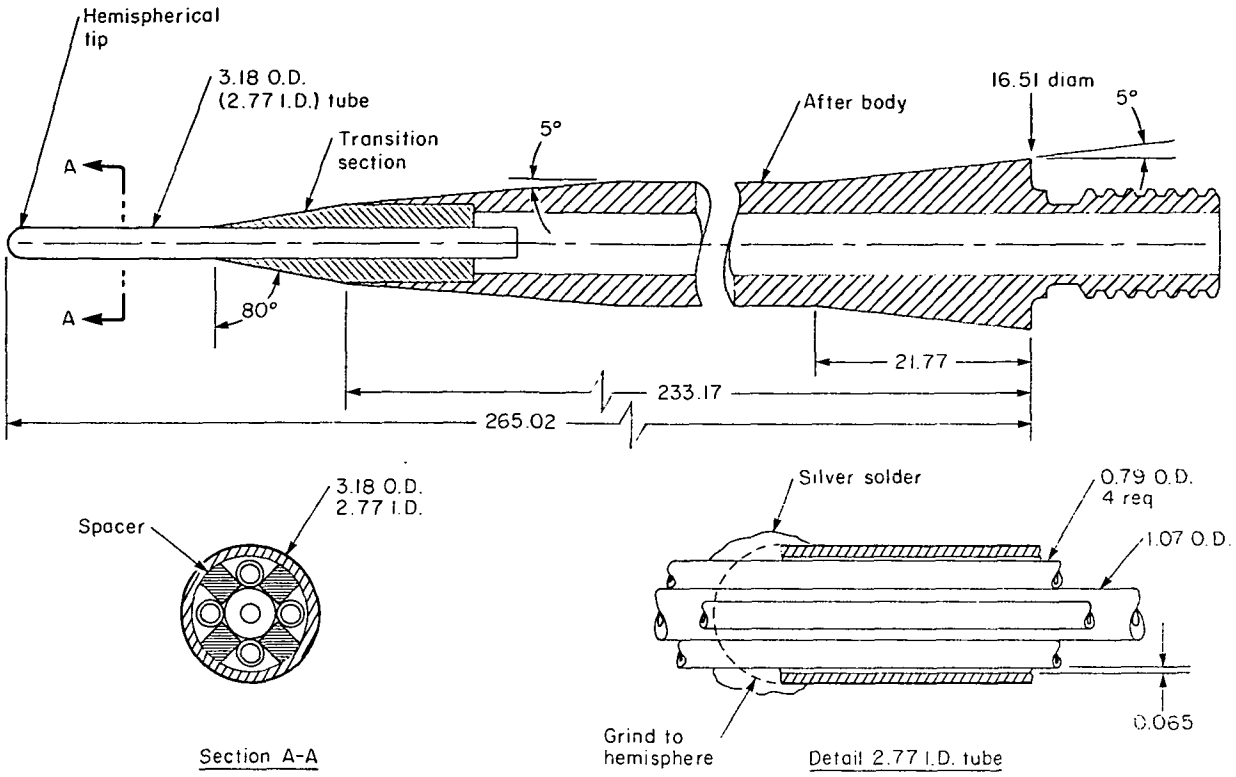

I.D. of all tubes 0.48

All dimensions in mm, unless otherwise noted.

Figure 1.- Flow-angle probe.

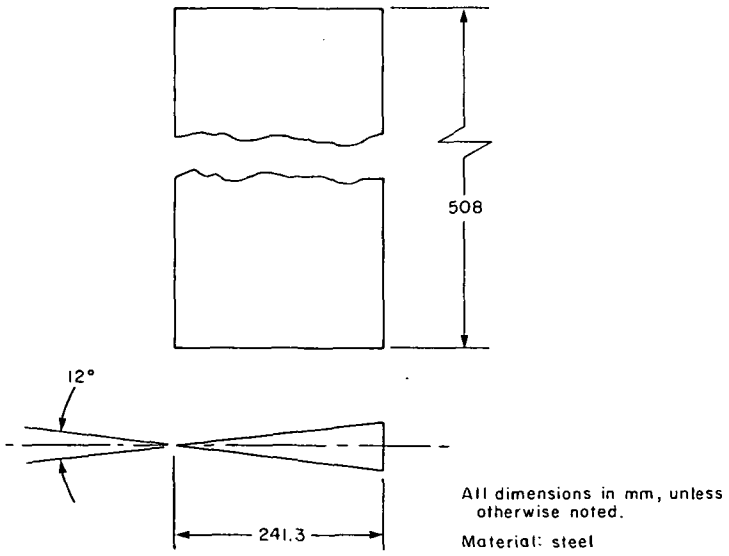

Figure 2.- 6° (half angle) wedge.

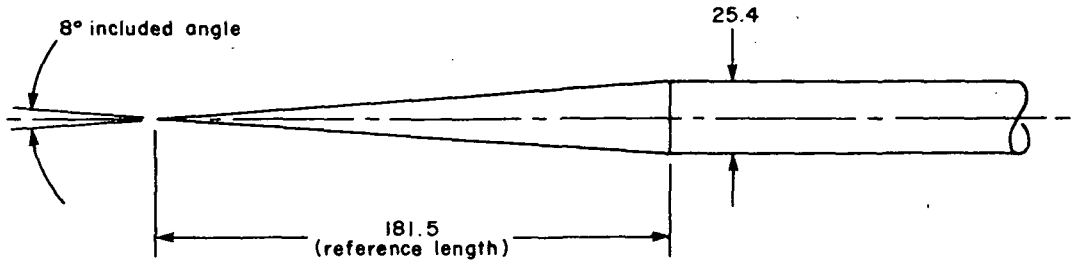

All dimensions in mm, unless otherwise noted.

Material: steel

Figure 3.- 4° (half angle) cone cylinder.

Wing area = 0.00506 m^2 (7.85 $in.^2$)

Wing span = 0.254 m (10.00 in.)

Horizontal tail span = 0.081 m (3.20 in.)

Material: steel

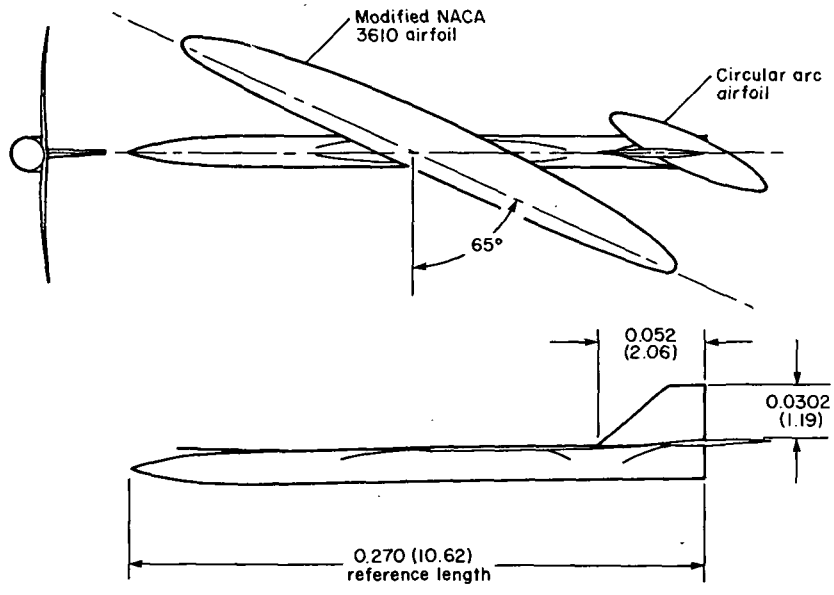

Note: All dimensions are in meters (inches), unless otherwise noted.

Figure 4.- Oblique-wing transport model.

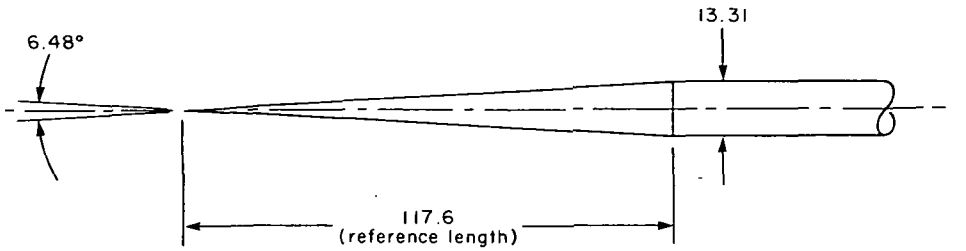

All dimensions in mm, unless otherwise noted.

Material: steel

Figure 5.- 3.24° (half angle) cone cylinder.

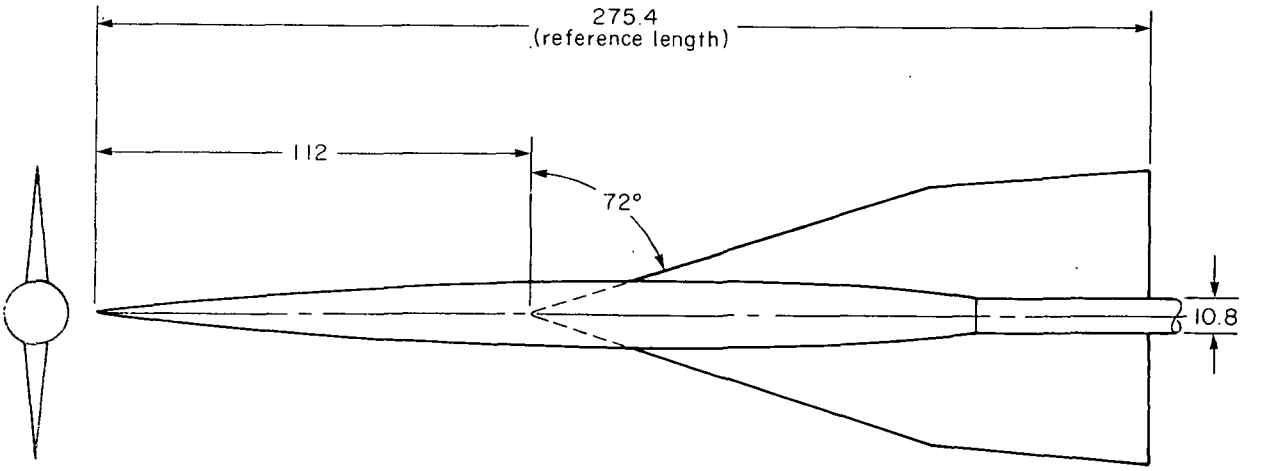

All dimensions in mm, unless otherwise noted.

Figure 6.- Clipped-tip delta-wing/body model.

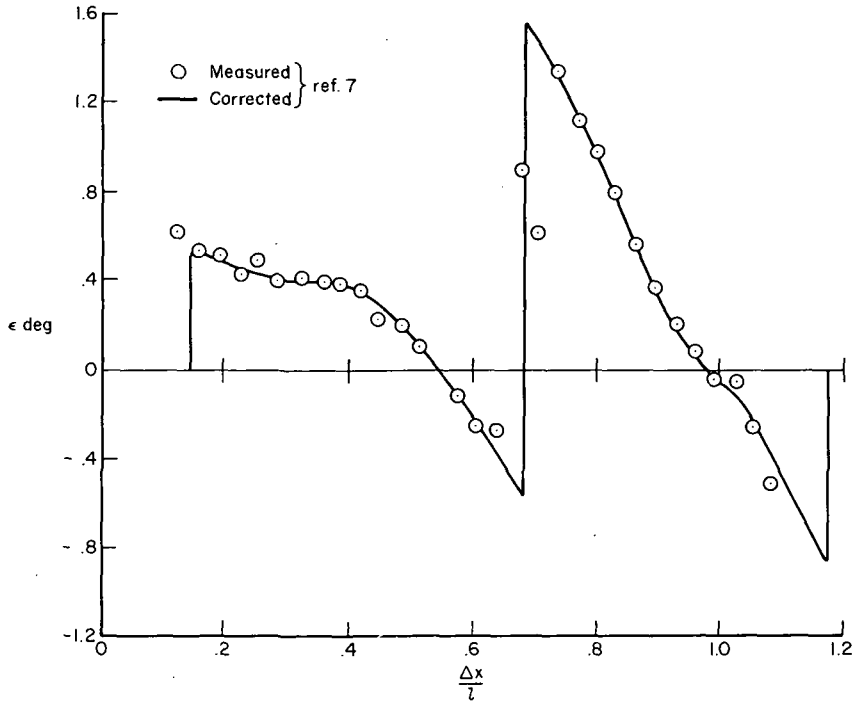

Figure 7.- Downwash angles (reproduced from ref. 7) for the clipped-tip delta-wing/body model, at M = 2.7; α = 2.6°, and h/l = 0.56.

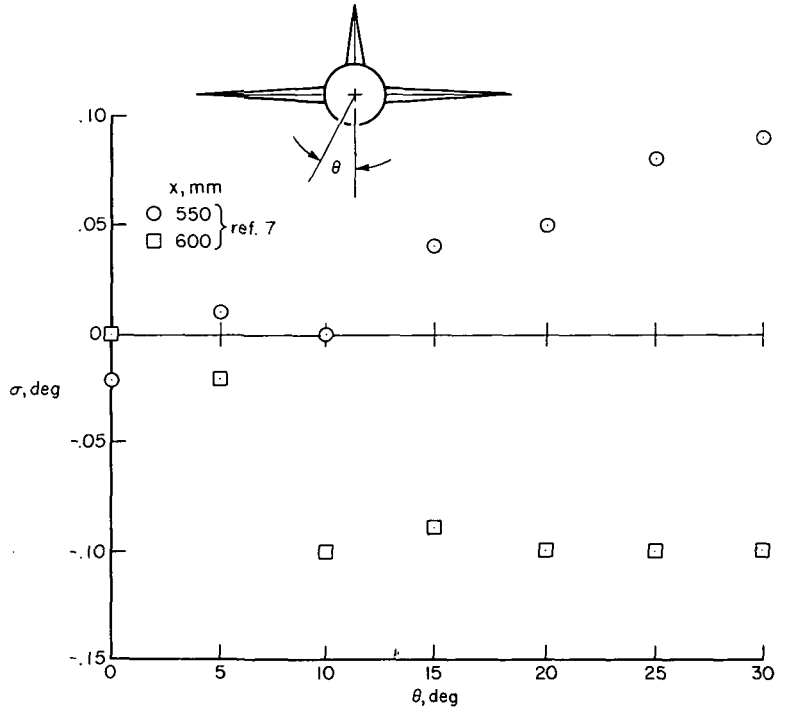

Figure 8.- Typical angles of sidewash for the clipped tip delta-wing/body model at M_∞ = 2.7, α = 2.6°, and h/l = 0.56.

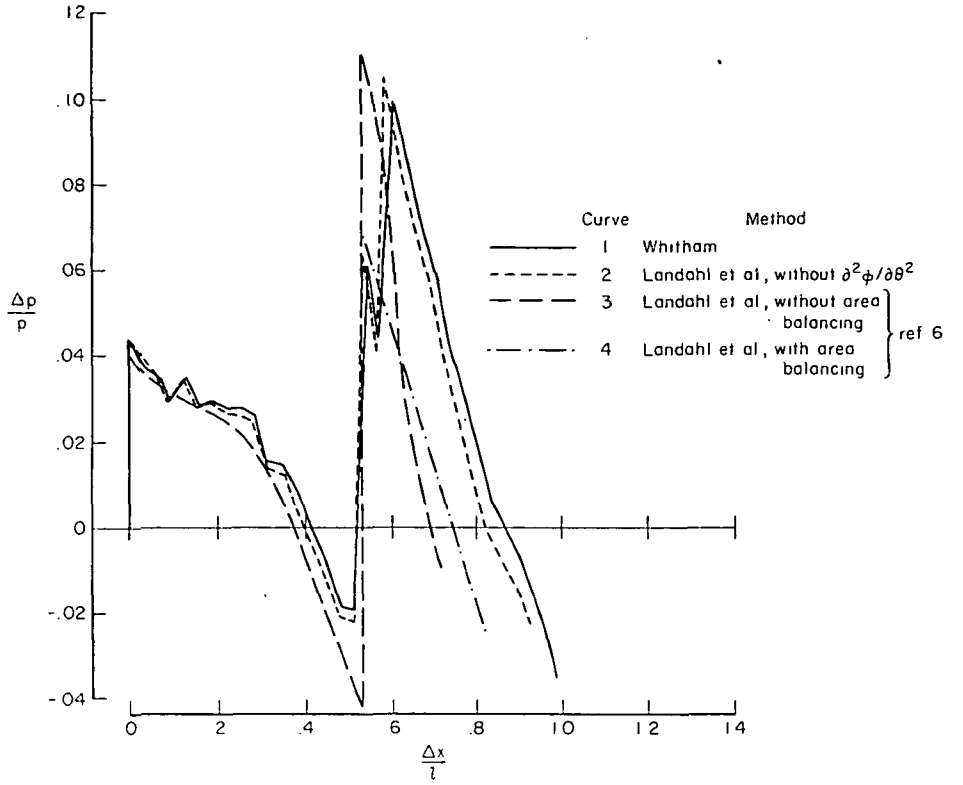

Figure 9.- Pressure signatures of the clipped-tip delta-wing/body model at $M_\infty = 2.7$, $\alpha = 2.60$, $h/l = 0.56$, and $\theta = 0°$.

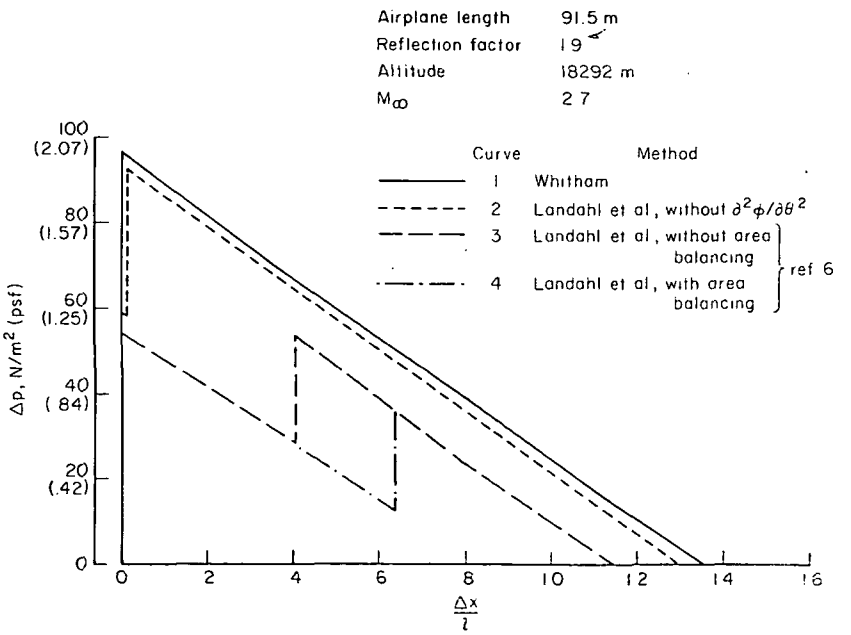

Figure 10.- Ground-pressure signatures extrapolated from data measured at $h/l = 0.56$, using the method of reference 12, for $\theta = 0°$.

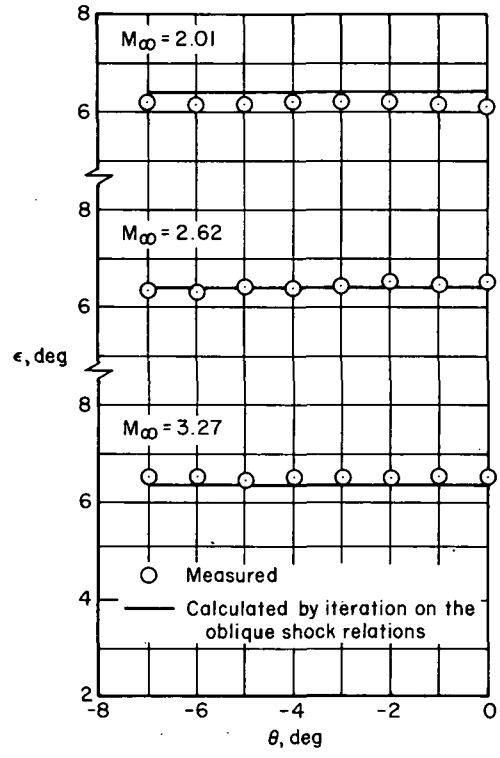

Figure 11.- Flow-angle measurements for the 6° (half angle) wedge.

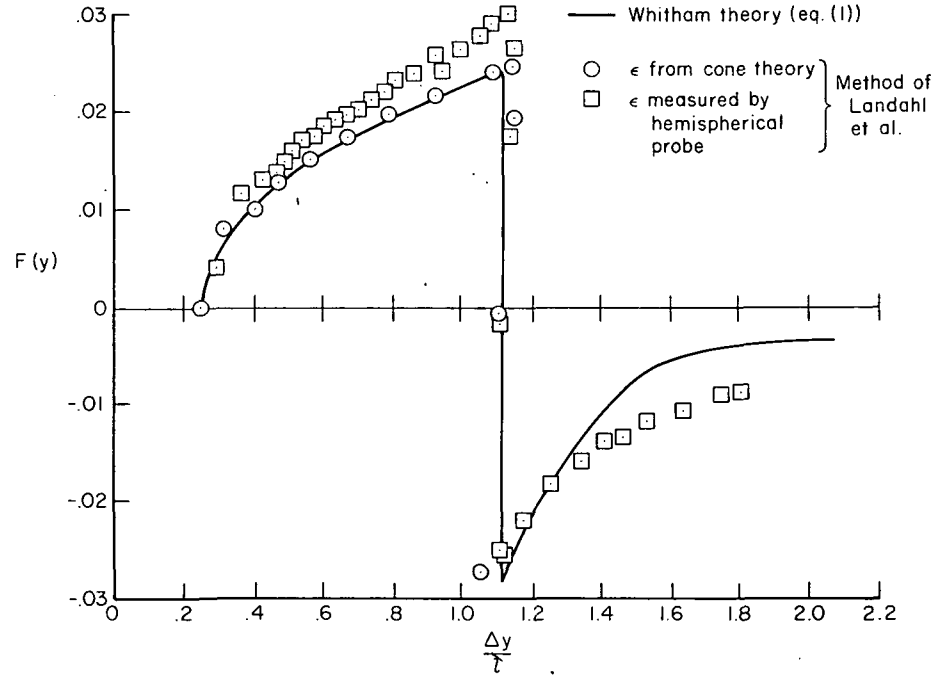

Figure 12.- F-functions for a 4° (half angle) cone cylinder calculated by the theories of Whitham and Landahl *et al.*, at $M_\infty = 2.01$.

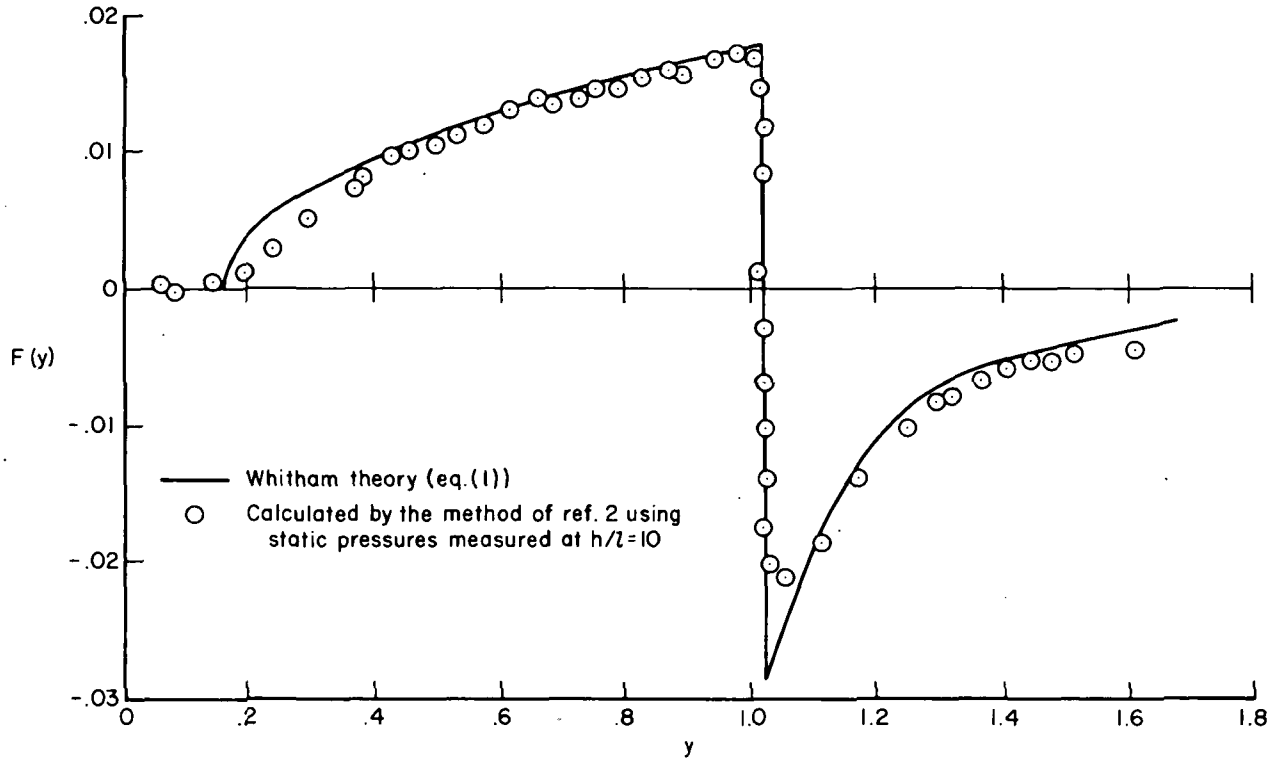

Figure 13.- F-functions for the 3.24° (half angle) cone cylinder at M_∞ = 1.68.

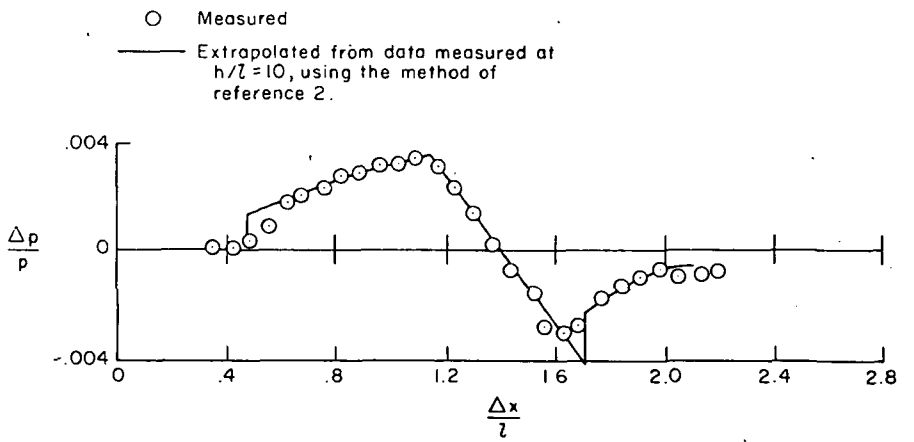

Figure 14.- Pressure signatures for a 3.24° (half angle) cone cylinder at M = 1.68 and h/l = 20.

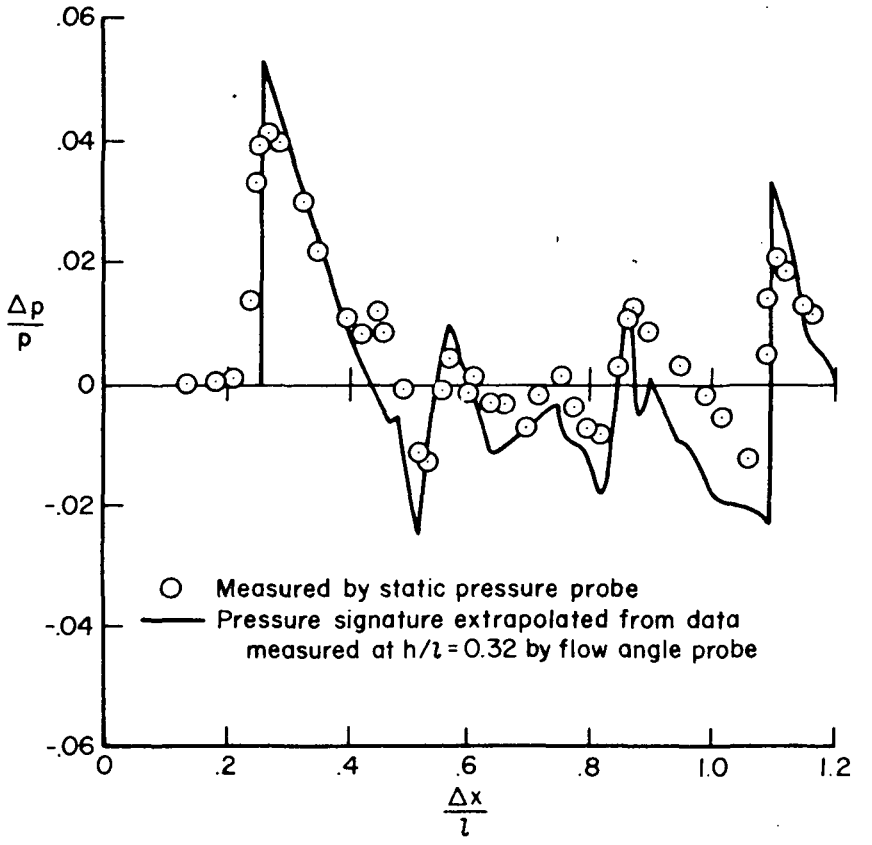

Figure 15.- Pressure signatures for the oblique-wing transport model at $M_\infty = 2.01$, $\alpha = 0^\circ$, and $h/l = 0.87$.

NATIONAL AERONAUTICS AND SPACE ADMINISTRATION
WASHINGTON, D.C. 20546

OFFICIAL BUSINESS
PENALTY FOR PRIVATE USE $300

SPECIAL FOURTH-CLASS RATE
BOOK

POSTAGE AND FEES PAID
NATIONAL AERONAUTICS AND
SPACE ADMINISTRATION
451

U.S.MAIL

POSTMASTER: If Undeliverable (Section 158 Postal Manual) Do Not Return

"The aeronautical and space activities of the United States shall be conducted so as to contribute . . . to the expansion of human knowledge of phenomena in the atmosphere and space. The Administration shall provide for the widest practicable and appropriate dissemination of information concerning its activities and the results thereof."

—NATIONAL AERONAUTICS AND SPACE ACT OF 1958

NASA SCIENTIFIC AND TECHNICAL PUBLICATIONS

TECHNICAL REPORTS: Scientific and technical information considered important, complete, and a lasting contribution to existing knowledge.

TECHNICAL NOTES: Information less broad in scope but nevertheless of importance as a contribution to existing knowledge.

TECHNICAL MEMORANDUMS: Information receiving limited distribution because of preliminary data, security classification, or other reasons. Also includes conference proceedings with either limited or unlimited distribution.

CONTRACTOR REPORTS: Scientific and technical information generated under a NASA contract or grant and considered an important contribution to existing knowledge.

TECHNICAL TRANSLATIONS: Information published in a foreign language considered to merit NASA distribution in English.

SPECIAL PUBLICATIONS: Information derived from or of value to NASA activities. Publications include final reports of major projects, monographs, data compilations, handbooks, sourcebooks, and special bibliographies.

TECHNOLOGY UTILIZATION PUBLICATIONS: Information on technology used by NASA that may be of particular interest in commercial and other non-aerospace applications. Publications include Tech Briefs, Technology Utilization Reports and Technology Surveys.

Details on the availability of these publications may be obtained from:

SCIENTIFIC AND TECHNICAL INFORMATION OFFICE

NATIONAL AERONAUTICS AND SPACE ADMINISTRATION

Washington, D.C. 20546